Catalysis Today 147S (2009) S198–S203

Contents lists available at ScienceDirect

Catalysis Today

journal homepage: www.elsevier.com/locate/cattod

A microstructured reactor/heat-exchanger for the water–gas shift reaction operated in the 533–673 K range

Anton R. Dubrovskiy [a,b], Evgeny V. Rebrov [b,*], Sergey A. Kuznetsov [a], Jaap C. Schouten [b]

[a] Tananaev Institute of Chemistry, Kola Science Centre RAS, 14 Fersman Street, 184209 Apatity, Murmansk region, Russia
[b] Department of Chemical Engineering and Chemistry, Eindhoven University of Technology, P.O. Box 513, 5600 MB Eindhoven, The Netherlands

ARTICLE INFO

Article history:
Available online 6 August 2009

Keywords:
Water–gas shift
Molybdenum carbide
Microreactor
Temperature profile
Modeling

ABSTRACT

A novel microstructured reactor/heat exchanger (MRHE) containing eight sections with each a cross-section of 10 mm × 10 mm and a length of 100 mm has been designed and constructed based on the kinetic model taken from Rebrov et al. [E.V. Rebrov, S.A. Kuznetsov, M.H.J.M. de Croon, J.C. Schouten, Catal. Today 125 (2007) 88]. Each section of the reactor compartment contains flat, perforated Mo plates and Mo wires with a diameter of 250 μm and a length of 100 mm coated with a porous Mo_2C layer. In the MRHE, the reactant mixture enters at 673 K and follows the optimal temperature profile which allows to minimize the reactor volume as compared with isothermal operation. The anode fuel cell gas preheated to 533 K is used as a coolant. Two coolant side streams are required to approach the optimal temperature profile in a counter-current MRHE. The start-up time required to heat the MRHE up to the operational temperature does not exceed 2 min.

© 2009 Elsevier B.V. All rights reserved.

1. Introduction

1.1. Water–gas shift reaction

For portable and transport applications, the most convenient and economical way of hydrogen production is on-board reforming of hydrocarbon fuels in a fuel processor (FP) combined with a fuel cell (FC) stack, forming an integrated power supply device. Space demand is a critical issue for medium and large sized applications ranging from 1 to some 10 kW. The fuel determines the operating temperature of the reforming process, which in turn determines the CO concentration in the reformate gas. In the reforming of gasoline or natural gas, a hydrogen-rich gas is produced at temperatures above 973 K with a carbon monoxide concentration of 5–12 vol.%. Because CO is a poison for a proton exchange membrane FC catalyst, the water–gas shift (WGS) reaction is used to reduce its concentration to below 1 vol.%, thereby increasing the H_2 yield. The application of an isothermal microreactor for the WGS reactor in fuel processing applications was demonstrated in [1]. This was already a substantial step ahead as compared with a conventional adiabatic WGS reactor consisting of two stages: the high and low temperature shift, with a heat exchanger in between. Here microtechnology may bring even more substantial benefit, as an integrated micro-structured reactor/heat exchanger (MRHE) offers an opportunity to perform the reaction in a single device and an internal temperature gradient shifts the thermodynamic equilibrium in the desired direction [2].

The concept of integrated reactors/heat exchangers was first proposed by Eigenberger and co-workers for coupling of methane steam reforming with methane combustion in meso-scaled reactors made from ceramic monoliths and steel foils [3–5]. The implementation of a declining temperature gradient into the WGS reactors by counter flow cooling has been realized for various systems up to 2 kW FC power range [6]. In those designs, a single coolant injection port was used which resulted in an almost linear temperature drop from 673 to 523 K along the reactor. However, an optimal temperature profile has a concave shape, which cannot be created by a counter-current operation. To approach an optimal temperature profile, several side ports for the coolant are required. Recently we demonstrated that a concave temperature profile can result in a more than twofold decrease of the catalyst volume on Mo_2C/Mo coatings in the WGS reactor [2]. The preferential oxidation of carbon monoxide (PrOx) is an exothermic reaction, where the operating temperature of the catalyst needs to be kept in a narrow range to achieve optimum selectivity. Thus, removing the heat generated by this chemical reaction is used to preheat the anode FC off-gas which is also used as coolant in the WGS MRHE, substantially decreasing its size.

1.2. Microreactor development

A water–gas shift catalyst for an automotive fuel processor should demonstrate sufficient activity in the temperature window between the reformer and PrOx reactors, have at least 5000 h

* Corresponding author.
E-mail address: e.rebrov@tue.nl (E.V. Rebrov).

0920-5861/$ – see front matter © 2009 Elsevier B.V. All rights reserved.
doi:10.1016/j.cattod.2009.07.037

stability, be non-pyrophoric, and provide a fast start-up. A commercial Cu–ZnO–Al_2O_3 catalyst has been used between the operating temperatures of 453 and 523 K. The temperature stability is poor above 523 K and it is pyrophoric if exposed to air. The catalytic coatings are usually deposited by wash-coating on the inner walls of the microchannels [7]. Recently developed Mo_2C catalysts showed a higher activity in the WGS reaction as compared with the commercial Cu/ZnO/Al_2O_3 catalyst [8]. They have also high stability against oxidation under reaction conditions, and do not catalyze the methanation reaction at elevated temperatures [9,10]. The surface area of Mo_2C catalysts can be increased by doping with Co or Ni [11,12]. However, the activity of Co (or Ni) doped Mo_2C catalysts in the WGS decreased in the course of the reaction due to sintering.

The catalytic activity of the Mo_2C/Mo coatings was determined in the WSG reaction in [2] to provide data for the reactor design. The reaction was conducted under the following conditions: P_{CO} = 300 Pa, $P_{H_2O} = 2.7$ kPa, $P_{CO_2} = 1.35$ kPa, $P_{H_2} = 5.65$ kPa, He as the balance, and a flow rate of 50 cm^3/min. The total pressure at the reactor outlet was 1 bar. The Mo_2C coatings were synthesized on flat and perforated molybdenum plates (99.9 wt.% Mo, 100 mm × 10 mm, with a thickness of 0.1 mm) and molybdenum wires with a diameter of 250 μm by galvanostatic electrolysis in a NaCl-KCl-Na_2MoO_4-Li_2CO_3 molten salt at 1123 K for 5.5 h with a cathodic current density of 5 mA/cm^2. The details of the synthesis method are described elsewhere [13].

In the development of an MRHE for the WGS reaction, several issues have to be considered such as the reactor material, the reactor lengths, catalyst production techniques, and microreactor fabrication methods. Compact microstructured heat exchangers, with triangular-sectioned passages, produced by stacking flat and perforated metal plates, are characterized by high ratios of heat-transfer surface area to core volume and considerably smaller fabrication costs than those with two sets of semi-cylindrical or rectangular channels machined on the opposite sides of a heat exchange plate. The volume between perforated and flat plates can be further utilized by insertion of a metal wire which splits the large triangular channel into three smaller channels whose geometry can be satisfactory described by equilateral triangles. The existence of sharp corners for the triangle significantly affects the flow patterns and hence the average heat and mass transfer coefficients relative to those for the circular or square sectioned channels. However, the water–gas shift reaction is relatively slow, and it always occurs under kinetic control even in channels with a larger hydraulic diameter as compared with that in this study. On the other hand, a decrease in heat transfer coefficient in triangular channels can be compensated by a larger heat-exchange area.

Numerical calculations performed in this study revealed that it is possible to achieve a temperature profile very close to the optimal one in a counter-current heat exchanger by cooling the reaction mixture with the anode fuel cell off-gas. It will be shown that at least two additional coolant streams should be mixed with the main coolant stream at specific positions. The proposed configuration has several advantages over the two-step process: (i) it is more compact because the total reactor volume is up to 50% smaller as compared with isothermal operation [2], and (ii) the water–gas shift is performed on the same catalyst which is inserted in a single housing eliminating the space required for connections and fittings between different reactors.

2. Microreactor/heat-exchanger design

The WGS reaction is an exothermic equilibrium reaction and the equilibrium conversion decreases with increasing temperature. Therefore, a significantly better performance can be achieved by operating at a relatively high temperature, thereby exploiting the reaction kinetics when the gas composition is far from equilibrium, and then lowering the temperature as thermodynamics begin to limit the CO conversion. The optimal temperature profile for the Mo_2C/Mo catalysts was calculated in [2]. The reactor temperature decreases along the reactor length from 673 to 533 K (Fig. 1).

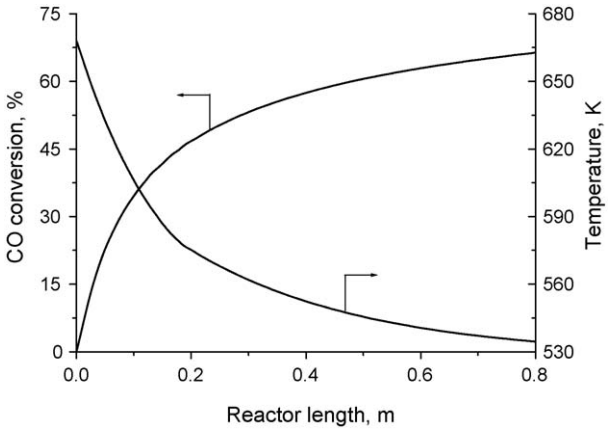

Fig. 1. The optimal temperature profile providing the highest WGS rate at corresponding axial positions in the 530–670 K temperature range and CO conversion on the Mo_2C/Mo catalyst: Reaction conditions: P_{CO} = 3.0 kPa, P_{H_2O} = 27.0 kPa, $P_{CO_2} = 13.5$ kPa, $P_{H_2} = 56.5$ kPa. Total flow: 750 cm^3 min^{-1} (STP). Mo_2C weight: 79.4 g.

The MRHE prototype module was designed for a total flow towards a fuel cell (FC) of 750 ml/min (STP) with outlet concentrations of CO and H_2 of 1.0 and 58 vol.%, respectively. This corresponds to a power generation in an FC of 45 W_e. Therefore, the WGS MRHE prototype represents a $^1/_{22}$ part of a 1 kW FC system which can be assembled by numbering-up of individual units as designed in this study.

Based on the reaction kinetics from [2], it was found that 74.9 g of Mo_2C coating is required to obtain the desired CO conversion of 66%. While this coated catalyst can be distributed in the microreactor part of the MRHE in different ways, several conditions related to the coating manufacturing method and the required temperature gradient of 140 K should be fulfilled. The heat conductivity of the reactor housing and its cross-section determine the axial thermal flux which levels out the temperature in the MRHE. Therefore, there exists a minimum reactor length which can still provide the desired temperature gradient. Another limitation is imposed on the width of a single Mo plate by the coating deposition method. The width is limited to 10 mm as wider plates require considerable adjustments in the deposition technique. The height of the reactor housing was also fixed at 10 mm to decrease the external surface of the MRHE prototype and to minimize the heat losses to the environment. Stainless steel 316 was chosen as a reactor housing material because this material is widely used in the production of microstructured reactors due to its excellent corrosion resistance and low costs. With an internal cross-section of 10 × 10 mm^2 and a wall thickness of 2 mm, the metal cross-section of the reactor housing is 9.6×10^{-5} m^2, which provides a heat transfer resistance (reactor length divided by metal cross-section and by metal thermal conductivity) of 650 K/W per 1 m of the reactor length. For the reactor length of 0.8 m, required to provide the desired catalyst loading, the mean heat flux in the metal will not exceed 6% of that to the coolant of 4.5 W at the temperature difference over the reactor length of 140 K. This value also allows to obtain a high heat recovery coefficient in the MRHE. The main parameters of the MRHE are summarized in Table 1. The reactor housing is formed by 8

Table 1
Design parameters of the microstructured reactor heat exchanger (MRHE).

Parameter	Value
Convective inlet heat flux (W)	19.9
Convective outlet heat flux (W)	15.9
Heat produced by the WGS reaction (W)	0.50
Heat removed by the coolant (W)	4.50
Heat conductivity of the reactor housing (W/m/K)	16
Metal cross-section of the reactor housing (m^2)	9.6×10^{-5}
MRHE length (m)	0.8
MRHE width (m)	0.01
MRHE height (m)	0.01
Reactor section volume (m^3)	8.0×10^{-5}
Mo_2C coating mass in the reactor (g)	74.9
Mo_2C coating volume (m^3)	2.0×10^{-5}
Solid fraction (Mo_2C and Mo) in the reactor (–)	0.746
Reaction mixture linear velocity (m/s)	0.492

sections with a length of 0.105 m each. Each reactor section is filled with eighteen perforated, seventeen straight Mo_2C/Mo plates, and Mo wires. Each Mo wire splits a large triangular channel to two smaller channels to form 576 triangular microchannels in each section of the microreactor. To avoid heat transfer by conduction via the catalytic plates, the length of the catalytic plates was a few millimeters smaller than that of corresponding reactor sections. The Mears criterion for laminar flow in a tube [2] was 0.006 and thus no external mass transfer limitations are to be expected.

3. Heat transfer modeling

3.1. 1D heat transfer model with mixing

Once the reactor dimensions were fixed, a one-dimensional heat transfer model has been applied to describe the temperature profile in the MRHE under the following assumptions, which are considered to be acceptable for the scope of this work:

(1) steady-state conditions;
(2) fully developed laminar flow;
(3) heterogeneous reaction at the catalytic wall in the reaction channels with kinetics taken from [2];
(4) constant physical properties of the reactant and coolant streams;
(5) constant enthalpy of the WGS reaction;
(6) uniform pressure along the MRHE channels;
(7) negligible axial diffusion in the gas phase.

These assumptions are based on the following calculations. The pressure drop in the reaction channels was neglected as it was below 5% from the outlet pressure. The physical properties of the reaction mixture did not change by more than 7% due to both the chemical reaction and temperature gradient. The entrance length was below 3% from the total channel length for both the reaction and cooling channels. The 1D model is based on lumping of both cross-sectional and peripheral distributions of variables. Under such an approximation, the gas–solid fluxes of heat and mass are assumed to be proportional to the difference of the gas-phase and wall average values of temperature and concentration.

The model calculates the temperature profiles of the reaction mixture flow (T_r), of three coolant flows (T_{c1}, T_{c2}, and T_{c3}), and of the reactor housing (T_m), which is in closed contact with the catalyst plates. Two side streams of the cold coolant combine with the preheated coolant entering the heat exchanger at x = 0.8 m and act as additional heat sinks in the overall heat exchange. As the flow rate of the coolant side stream increases, the temperature of the mixed coolant stream decreases and vice versa. The mixing of the coolant streams was modeled using a 2D model which resembles the geometry of T-mixers and the side coolant stream flows in them. The mixing was determined in the 2D model by recording the coolant temperature over the channel cross-section. The 2D model allowed to calculate the thermal mixing length required for temperature equalization over the cooling channel cross-section. Then, empirical mixing coefficients were introduced in the 1D heat transfer model in order to match the coolant temperature profiles in the 1D model to those in the 2D model. Thus, the temperature profile of the gases is determined by convective heat transport, heat exchange with the reactor housing, heat transfer in the reactor housing by conduction, and the position of the coolant side stream injection ports.

The computational domain in the 1D model was divided into three subdomains as the coolant flow was different in those parts due to two additional coolant injections whose positions were varied in order to get the minimum deviation from the optimal temperature profile shown in Fig. 1. When the length coordinate is made dimensionless with the length of the reactor, the equation for the reaction mixture flow is invariable of all three subdomains:

$$(\dot{m}C_p)_r \frac{dT_r}{d\hat{x}} = -\alpha_r A_r (T_r - T_m) + |\Delta_r H| r \tag{1}$$

where $(\dot{m}C_p)_r$ is the heat transport capacity (mass flow rate - × specific heat capacity) of the reactant flow, α_r is the gas–solid heat transfer coefficient, A_r is the respective heat exchange surface area, $\Delta_r H$ is the enthalpy of the WGS reaction, and r is the WGS reaction rate. The mass balance equations were solved together with the equation for the ideal temperature profile (2) to obtain concentration profiles.

$$\frac{dT_{id}}{d\hat{x}} = -22 - 661 \cdot e^{-5.9\hat{x}},\ T_{id}(\hat{x} = 0) = 668\ \mathrm{K} \tag{2}$$

The CO concentration profile is shown in Fig. 1. It should be mentioned that the heat released due to the WGS reaction (0.49 W) adds up only 11% to the total amount of heat transferred to the cooling channels (4.50 W). The small changes in the temperature profile during optimization of the positions of the coolant side ports (see Section 3.2) resulted in the maximum deviation of heat released due to the reaction of 0.12 W or 2.7% in terms of the total amount of heat transferred to the coolant. Therefore, the changes in the reaction rate due to a deviation from the ideal temperature profile were not considered in the heat transfer model, while the heat released due to the reaction was taken into account via a heat generation term (3).

$$\dot{Q}(r) = |\Delta_r H| r = |\Delta_r H| C^0_{CO} \upsilon \cdot \frac{dX_{CO}}{d\hat{x}} = |\Delta_r H| F^0_{CO} \frac{dX_{CO}}{d\hat{x}} = \dot{Q}_{tot} \frac{dX_{CO}}{d\hat{x}}, \tag{3}$$

where C^0_{CO} is the inlet CO concentration, υ is the total reactant flow, F^0_{CO} is the molar CO flow, and $X_{CO} = C^0_{CO} - C_{CO}/C^0_{CO}$ is the CO conversion. The heat generation term can be replaced by a fitting function, which is a function of the axial reactor position only (4):

$$\dot{Q}(\hat{x}) = \dot{Q}_{tot} X^{out}_{CO} \cdot (A1 \cdot (1 - A2 \cdot e^{-A3\hat{x}})) \tag{4}$$

where X^{out}_{CO} is the CO conversion at the reactor outlet. Fitting parameters A1–A3 are normalized to obtain $1/\dot{Q}_{tot} X^{out}_{CO} \int_0^1 \dot{Q}(\hat{x}) d\hat{x} = 1$. This gives the following values of parameters: A1 = 0.301, A2 = 22, and A3 = 9.5.

Taking into account the counter current flow regime with two side stream injections, the temperatures of the first, second, and

third coolant stream are described by the following differential equations,

$$(\dot{m}C_p)_{c1}\frac{dT_{c1}}{d\hat{x}} = \alpha_c A_c(T_m - T_{c1}) + \sum_{j\neq i}\xi_{1j}(T_{c1} - T_{cj})$$
$$(\dot{m}C_p)_{c2}\frac{dT_{c2}}{d\hat{x}} = \alpha_c A_c(T_m - T_{c2}) + \sum_{j\neq i}\xi_{2j}(T_{c2} - T_{cj}) \quad (5)$$
$$(\dot{m}C_p)_{c3}\frac{dT_{c3}}{d\hat{x}} = \alpha_c A_c(T_m - T_{c3}) + \sum_{j\neq i}\xi_{3j}(T_{c3} - T_{cj})$$

where $(\dot{m}C_p)_i$ is the heat transport capacity (mass flow rate - × specific heat capacity) of coolant flow i, α_i is the gas–solid heat transfer coefficient, A_i is the respective heat exchange surface area, and ξ_{ij} are the empirical mixing coefficients which describe the rate of temperature equalization after injection of a coolant side stream (see Table 2). It was found that the temperature equalization occurs at a distance of 20 channel diameters from the T-mixer during mixing of the first and second cooling streams (Fig. 2), while it happens within 10 channel diameters during mixing of the first and second cooling streams with the third one. This behavior can be described in the 1D model with the same value of the mixing coefficients of 1 (see Table 2).

The reactor housing temperature (T_m) is described by Eq. (3),

$$-\frac{\lambda_m A_m}{L}\frac{d^2T_m}{d\hat{x}^2} = \alpha_r A_r(T_r - T_m) - \alpha_c A_c(3T_m - T_{c1} - T_{c2} - T_{c3}), \quad (6)$$

where λ_m is the conductivity of the reactor material, A_m is the cross-sectional area of the reactor housing, and L is the MRHE length. The values of the key design parameters are listed in Table 1. Both Shah [14] and Baliga and Azrak [15] concluded that the average Nusselt number for the convective fully developed laminar flow, in a triangular duct under constant heat flux boundary conditions, is equal to 3.11, if no rounded corners are present in the geometry. However, the geometry applied in this study contains one rounded corner substantially enhancing the heat transfer rate. In this case, the Nusselt number equals 3.40 [16]. This value was used in this study for the triangular reaction channels formed by the perforated plate, the flat plate and a wire, to calculate the heat transfer coefficient (α_r) in the reaction channels. In the cooling channels, a constant Nusselt number of 4.36 was applied [16].

An investigation of the overall heat transfer coefficient in the integrated MRHE showed that a key heat transfer constraint was the heat transfer coefficient between the wall surface and the coolant flow. The heat transfer by conduction in the radial direction was much faster; therefore, the temperature gradient between the inner and outer sides of the metal housing was below 1 K. To maximize the heat-exchange area required for an efficient heat removal, two parallel tubes with circular cross-sections were positioned on a side wall of the MRHE.

Table 2
Values of the mixing coefficients in the 1D heat transfer model in the first and second subdomains (Eq. (2)).

	Subdomain 1			Subdomain 2		
Dimensions, m	x = [0-P1]			x = [P1-P2]		
Equation	$\xi i1$	$\xi i2$	$\xi i3$	$\xi i1$	$\xi i2$	$\xi i3$
T_{c1}	0	−1	−1	0	−1	0
T_{c2}	1	0	−1	1	0	0
T_{c3}	1	1	0	0	0	0

P1 and P2 are the injection positions of coolant side streams (design parameters). See Fig. 3 for their definition. In subdomain 3 (x = [P2-0.8]) ξ_{ij} = 0.

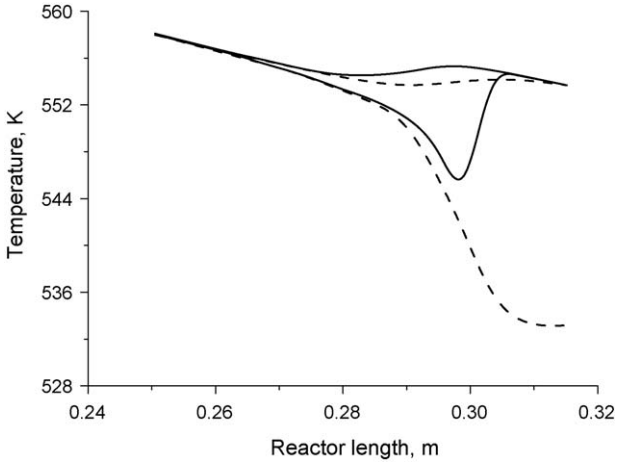

Fig. 2. Comparison between 1D (dashed lines representing the main and side coolant streams) and 2D (solid lines representing minimum and maximum temperatures) heat transfer models in the T-mixer. 2D model was composed of Navier–Stokes equations, where the coolant side stream was mixed with the main coolant stream at an angle of 90°. The 1D model was composed by Eqs. (1) to (3). The values of the mixing coefficients ξ_{ij} were fitted in order to minimize the differences in the coolant temperatures between the 1D model and the 2D model (see Table 2).

3.2. Optimization of the positions of coolant side stream ports

The effect of two design parameters was investigated in the optimization of the temperature profile: the positions of the first (P1) and second (P2) coolant side stream ports (see Fig. 3). The mean-square deviation from the desired temperature profile was chosen as the objective function

$$\delta(\%) = \frac{1}{T_{av}}\sqrt{\frac{1}{99}\sum_{j=1}^{100}(T_{opt(j)} - T_j)^2 \cdot 100} \quad (7)$$

where $T_{opt(j)}$ and T_j are the temperatures of the reaction mixture at j point of the optimal temperature profile and simulated, respectively; T_{av} is the average temperature of the reaction mixture. Fig. 4 demonstrates the mean-square deviation of the simulated temperature profiles of the reaction mixture from the optimal temperature profile as a function of the positions of the coolant side stream ports. There is a minimum in the objective function at P1 of 0.3 m and P2 of 0.125 m from the reaction mixture inlet. The corresponding coolant distribution between the three streams is given in Table 3. It is not possible to approach the optimal

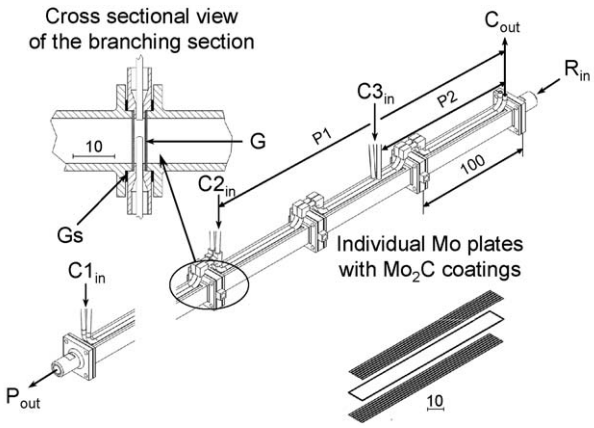

Fig. 3. A schematic view of the microstructured reactor/heat exchanger (MRHE). P1 and P2 are the positions of two coolant side stream ports relative to the reactant inlet, which is taken as x = 0. R_{in}—reaction mixture inlet, P_{out}—product outlet, $C1_{in}$—first coolant flow inlet, $C2_{in}$—second coolant flow inlet, $C3_{in}$—third coolant flow inlet, C_{out}—coolant outlet. All sizes are given in mm.

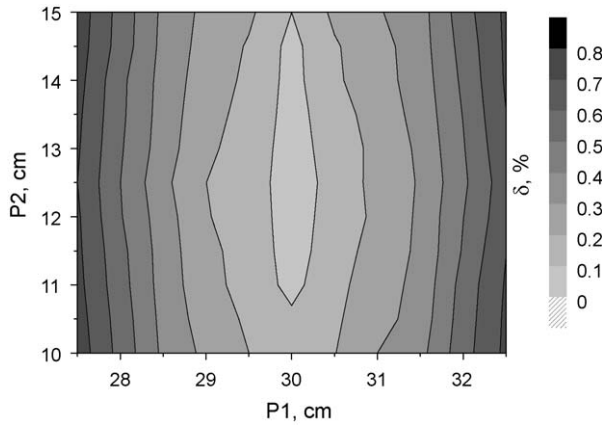

Fig. 4. The mean square deviation (δ, %) of the simulated temperature profiles from the optimal temperature profile as a function of the positions (P1 and P2) of the coolant side stream ports. The reactant and coolant flows for the minimum of the objective function are given in Table 3 and the corresponding temperature profiles are shown in Fig. 5.

Table 3
Flow conditions and corresponding heat fluxes in the MRHE.

	Inlet temperature, K	Outlet temperature, K	Heat transport capacity, W/K	Heat flux, W	Flow, cm^3/min (STP)
Reaction flow	673	537	0.0295		750
Coolant flow 1	533	610	0.0446	3.43	4000
Coolant flow 2	533	610	0.0127	0.98	1150
Coolant flow 3	533	610	0.0012	0.09	100
Coolant total				4.50	5250

temperature profile with a deviation less than 1% using only one single coolant side stream. However, with two coolant side streams, the deviation from the optimal temperature profile can be as low as 0.7%. The position of the second coolant flow inlet port should be exactly fixed at $x = 0.3$ m, while the position of the third coolant flow has a larger range of possible values, which should be taken into account during reactor assembling.

Fig. 5 shows the temperature profile of the reaction mixture in comparison with the optimal, and the temperature profile of all

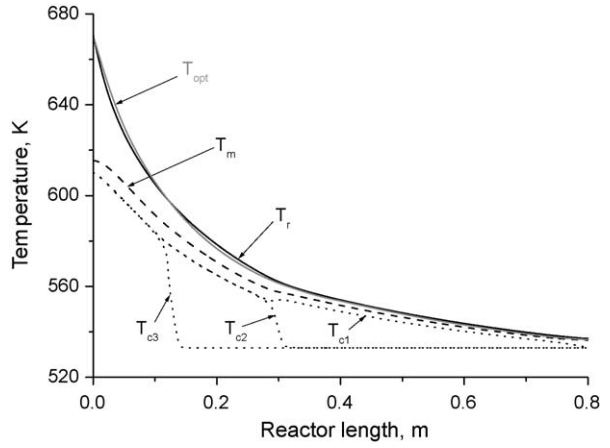

Fig. 5. Temperature as a function of the reactor length: optimal temperature providing the highest WGS rate (gray); reaction mixture temperature (T_r, black); reactor housing (T_m, dashed line); temperature of coolant flows (T_{c1}, T_{c2}, and T_{c3}, dotted lines).

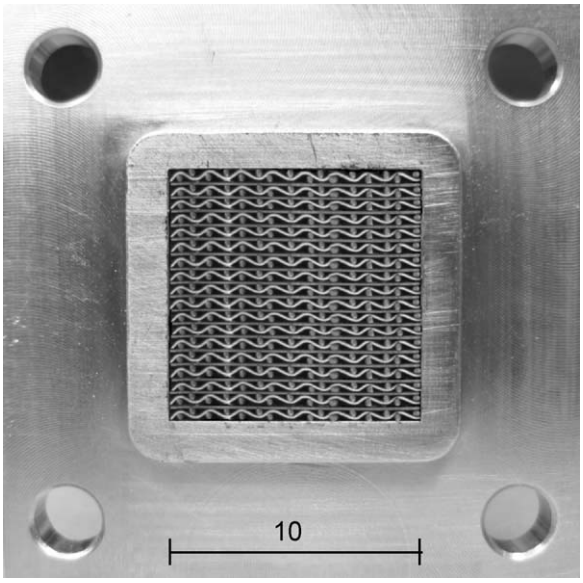

Fig. 6. A cross-sectional image of a single section of the MRHE with inserted flat, perforated Mo_2C/Mo plates and wires. The coolant channels are not seen in this view as they are behind the connecting flange. The scale bar is in mm.

coolant streams and the reactor housing obtained by the 1D model.

The volume of the present MRHE prototype of 0.08 L for a 45 W_e FC would lead to a volume of 80 L for a 45 kW FC stack of which 20 L is the catalyst volume (Fig. 6). The fresh industrial HT and LT WGS catalysts for a similar size of the FC occupy ca. 2 and 12 L, respectively, with an additional volume required for a heat exchanger, connecting pipes and flow distribution devises. Those parts assembled together occupy approximately the same volume as the present MRHE prototype based on the Mo_2C/Mo coatings. A high thermal stability of the Mo_2C/Mo catalyst allows to limit its loading up to a 5% surplus with respect to that required for CO removal. The activity of the Mo_2C/Mo catalyst remains stable for more than 5000 h time-on-stream, whereas the commercial Cu/ZnO/Al_2O_3 catalyst losses up to 30% of its initial activity for the same time interval. While the present design does not allow substantially decrease of the catalyst volume, it has several important advantages related to the start-up time and inherent safety of operation. It takes only 2 min in order to warm up the catalyst to the mean reaction temperature using a hot stream with the same flow rate as the coolant stream applied to create the required temperature gradient. Once the reactor is shut down, the housing temperature can be reduced within a similar time interval to below 350 K, after that the catalyst can be safely exposed to air. Furthermore, it is important to mention that the efficiency of a fuel processor can be substantially increased as the WGS MRHE reactor operates without substantial pressure drop which in turn allows to decrease the pressure in the reformer increasing the hydrogen yield.

It can be seen from Table 2, the required coolant flow is 5250 cm^3/min (STP) while the reactant flow is 750 cm^3/min (STP). The hydrogen conversion in a FC is usually 85–90% which corresponds to the anode exhaust gas flow rate in the range between 360 and 380 cm^3/min (STP). Therefore, the largest part of the coolant flow should be recycled to maintain the optimal temperature profile. After mixing with the cold anode gas, this flow can be sent back to the WGS MRHE as a coolant. This recycle loop can decrease the influence of variations in the temperature and composition of the anode off-gas during transient operation.

4. Conclusions

It is possible to create a temperature profile providing the highest rate of the WGS reaction over Mo_2C/Mo coatings along the length of a microstructured reactor/heat-exchanger. Two coolant side streams are required to approach the optimal temperature profile in a counter-current MRHE. The start-up time required to heat the MRHE up to the mean operational temperature does not exceed 2 min. In scaling up, it is desirable to form a stacked three-dimensional assembly (3D architecture) in preference to using larger planar sheets. This reduces the surface-to-volume ratio and thus the surface convective losses. The modular design of the MRHE developed in this study allows to fulfill the required production of hydrogen in several steps corresponding to a FC power output of 45 W_e with a single reactor module volume of 80 cm^3. The WGS MRHE was manufactured according to the proposed design. The computational results effectively demonstrate the potential of microreactor-based on-demand H_2 generation, and provide insights for a subsequent phase of development involving integrated WGS MRHE–PrOx–FC systems.

Acknowledgements

The financial support by the Netherlands Organization for Scientific Research (NWO), project No. 047.017.029, and by the Russian Foundation for Basic Research (RFBR), project No. 047.011.2005.016, is gratefully acknowledged.

References

[1] A.Y. Tonkovich, J.L. Zilka, M.J. LaMont, Y. Wang, R.S. Wegeng, Chem. Eng. Sci. 54 (1999) 2947.
[2] E.V. Rebrov, S.A. Kuznetsov, M.H.J.M. de Croon, J.C. Schouten, Catal. Today 125 (2007) 88.
[3] J. Frauhammer, G. Friedrich, G. Kolios, T. Klingel, G. Eigenberger, L. von Hippel, D. Arntz, Chem. Eng. Technol. 22 (1999) 1012.
[4] J. Frauhammer, G. Eigenberger, L. von Hippel, D. Arntz, Chem. Eng. Sci. 54 (1999) 3661.
[5] G. Kolios, J. Frauhammer, G. Eigenberger, Chem. Eng. Sci. 57 (2002) 1505.
[6] G. Kolb, J. Schürer, D. Tiemann, M. Wichert, R. Zapf, V. Hessel, H. Löwe, J. Power Sources 171 (2007) 198.
[7] R. Zapf, C. Becker-Willinger, K. Berresheim, H. Bolz, H. Gnaser, V. Hessel, G. Kolb, P. Löb, A.-K. Pannwitt, A. Ziogas, Trans. I Chem. E Part A 81 (2003) 721.
[8] J.S. Lee, S.T. Oyama, M. Boudart, J. Catal. 106 (1987) 125.
[9] J. Patt, D.J. Moon, C. Phillips, L. Thompson, Catal. Lett. 65 (2000) 193.
[10] S.A. Kuznetsov, A.R. Dubrovskiy, E.V. Rebrov, J.C. Schouten, Z. Naturforsch. V62a (2007) 647.
[11] M. Nagai, K. Matsuda, J. Catal. 238 (2006) 489.
[12] M. Nagai, A.Md. Zahidul, K. Matsuda, Appl. Catal. A 313 (2006) 137.
[13] A.R. Dubrovskiy, S.A. Kuznetsov, E.V. Rebrov, J.C. Schouten, V.T. Kalinnikov, Doklady Chem. 421 (2) (2008) 186.
[14] R.K. Shah, Int. J. Heat Mass Transfer 18 (1975) 849.
[15] B.R. Baliga, R.R. Azrak, ASME, J. Heat Transfer 108 (1986) 24.
[16] R.K. Shah, A.L. London, Laminar Flow Forced Convection in Ducts, Academic Press, New York, 1978.